Chinese Chemical Letters 31 (2020) 386–390

Contents lists available at ScienceDirect

Chinese Chemical Letters

journal homepage: www.elsevier.com/locate/cclet

Communication

A heteropore covalent organic framework for adsorptive removal of Cd(II) from aqueous solutions with high efficiency

Na Liu[a], Liangfeng Shi[a,b,1], Xianghao Han[b,1], Qiao-Yan Qi[b], Zong-Quan Wu[a,*], Xin Zhao[b,*]

[a] Department of Polymer Science and Engineering, School of Chemistry and Chemical Engineering, and Anhui Key Laboratory of Advanced Catalytic Materials and Reaction Engineering, Hefei University of Technology, Hefei 230009, China
[b] CAS Key Laboratory of Synthetic and Self-Assembly Chemistry for Organic Functional Molecules, Center for Excellence in Molecular Synthesis, Shanghai Institute of Organic Chemistry, Chinese Academy of Sciences, Shanghai 200032, China

ARTICLE INFO

Article history:
Received 7 May 2019
Received in revised form 18 June 2019
Accepted 27 June 2019
Available online 27 June 2019

Keywords:
Covalent organic frameworks
Heteropore
Hierarchical porosity
Cd(II) removal
Water treatment

ABSTRACT

A heteropore covalent organic framework (COF) integrating tetraphenylethene skeleton and catechol segment is designed and synthesized. It exhibits extremely high stability in water under different pH conditions, which makes it an excellent material for adsorptive removal of Cd(II) from aqueous solutions with very fast adsorption kinetics, high uptake capacity, and good recyclability.

Given the Earth's ever-increasing industrial and mining activities, heavy metals pollution, especially heavy metal ions pollution in water systems, pose a significant threat to the ecological environment and public health due to the fact that they are not biodegradable, highly toxic and can accumulate in living organisms [1]. As one of the harmful heavy metals, cadmium has been listed as a category-I carcinogen by the International Agency for Research on Cancer and as a group-B1 carcinogen by the US Environment Protection Agency (EPA). Cadmium is known to directly damage nervous, reproductive, renal and skeletal systems, and also to cause some diseases such as emphysema, kidney failure, itai–itai disease, hypertension, and testicular atrophy [2]. However, cadmium has a wide range of commercial uses, including batteries, electroplating, coating operations, television phosphors, *etc.* [3]. Unfortunately, the widespread applications often result in high pollution risks, especially in aquatic systems, in which levels of cadmium are dependent on sources [4]. To protect human health and the environment, there is an urgent need to develop effective technologies for removing cadmium from wastewater.

Over the past decades, various techniques have been developed to eliminate cadmium from wastewater discharges, which include precipitation [5], adsorption [6], membrane filtration [7], reverse osmosis [8], *etc.* Among these methods, adsorption has been proven to be an efficient one for water pollution remediation because of its relatively low cost, simple design, ease operation and regeneration. In this context, several types of adsorbent materials, including activated carbon [9], polymers [10], and metal-organic frameworks (MOFs) [11], have been developed for adsorptive removal of cadmium from contaminated water. However, these adsorbents face disadvantages such as low temperature and pH tolerance, low capacity, moderate affinity to Cd(II), which typically limit their practical applications. Therefore, it is highly desirable to develop robust porous materials to overcome the existing limitations.

Covalent organic frameworks (COFs) are a new class of crystalline porous polymers with a history dating back to 2005 [12]. Their well-defined network structures are connected by covalent bonds of light elements and have the advantages of low density, high thermal stability, well-ordered inside nanochannels, permanent porosity, high surface area, and designable functionality. Over the last decade, COFs have attracted considerable attention due to their promising applications in gas adsorption and separation, catalysis, sensing, optoelectronics, ion conduction, and energy storage [13]. On the other hand, the unique structural characteristics of COFs also make them attractive for applications in the removal of metal ions from wastewater. To this end, this potential has been explored very recently, which demonstrates that COFs are very promising in wastewater treatment [14]. However, compared with those designed to implement the

* Corresponding authors.
E-mail addresses: zqwu@hfut.edu.cn (Z.-Q. Wu), xzhao@sioc.ac.cn (X. Zhao).
[1] These authors contributed equally to this work.

https://doi.org/10.1016/j.cclet.2019.06.050
1001-8417/

aforementioned applications, COFs capable of adsorbing metal ions from aqueous solutions are far less explored. A major reason is that most structures of COF family are not robust enough to survive under the harsh (strongly acidic and basic) conditions usually encountered in wastewater treatment. To be a good adsorptive material for water purification, both high chemical stability and large adsorption capacity must meet simultaneously. We herein report the design and synthesis of a new dual-pore COF which is highly stable in water under neutral, acidic and basic conditions. Moreover, it can rapidly adsorb Cd(II) in aqueous solutions with an exceptionally high uptake capacity.

Since porous materials with hierarchical structures are advantageous to mass transport and diffusion [15], a heteropore COF, which displays heterogeneous porosity [16], was designed. To improve stability against harsh aqueous conditions, intramolecular hydrogen-bonding interaction is introduced into the skeleton of the designed COF by using 2,3-dihydroxybenzene-1,4-dicarbaldehyde(2,3-Dha) as a building block [17]. On the other hand, the *ortho*-dihydroxy group of the catechol moiety provides an open chelate site to bind to metal ions (Scheme 1). COF-ETTA-2,3-Dha was synthesized as a red powder by the condensation of 4,4′,4″,4‴ -(ethene-1,1,2,2-tetrayl)tetraaniline (ETTA) and 2,3-Dha in a mixed solvent of 1,4-dioxane/acetic acid (aq., 9 mol/L) (1:0.1, v/v) in a sealed glass ampoule at 120 °C for 72 h (Scheme 1b).

The as-prepared crystallites were firstly characterized using FTIR spectroscopy. While nearly complete disappearance of the peaks corresponding to C=O (1649 cm^{-1} of 2,3-Dha) and —NH_2 (3437 and 3353 cm^{-1}) indicates a high degree of polymerization by consuming almost all the aldehydes and amine groups of the monomers, a band assignable to the vibration of C=N is observed at 1615 cm^{-1}, giving direct evidence for the formation of imine linkages (Fig. S1 in Supporting information). The solid-state ^{13}C cross-polarization magic-angle-spinning (CP/MAS) NMR spectrum further confirms the presence of imine carbon in COF-ETTA-2,3-Dha which appears at 159.8 ppm (Fig. S2 in Supporting information). Thermogravimetric analysis (TGA) reveals that the COF possesses good thermal stability, as indicates by the less than 6% weight loss when the temperature increased from room temperature to 350 °C (Fig. S3 in Supporting information). The morphology of the COF was examined by scanning electron microscopy (SEM) and transmission electron microscopy (TEM), which showed a large number of hollow spherical structures with diameters around 2 μm (Fig. S4 in Supporting information).

In order to determine the crystal structure of the as-prepared COF, its PXRD pattern was recorded and compared with the simulated ones which were generated from the Accelrys Materials Studio software [18]. It should be noted that the combination of ETTA and 2,3-Dha theoretically would give rise to two possible framework structures, that is, a dual-pore (DP) COF and a single-pore (SP) COF (Fig. 1, bottom). Therefore, the two structures with eclipsed (AA) and staggered (AB) stackings which are the typical stacking models of 2D COFs, were constructed and their PXRD

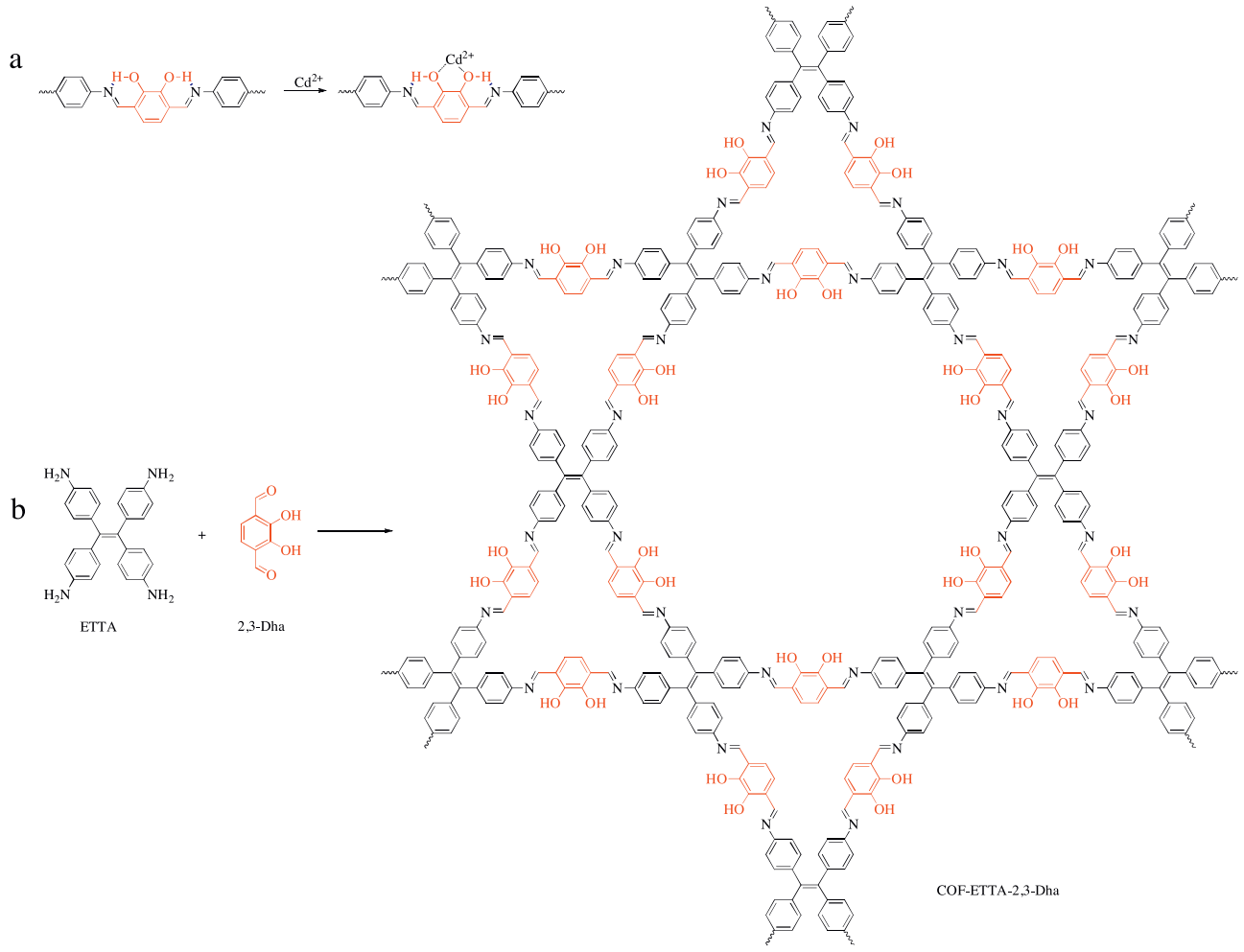

Scheme 1. (a) The model to illustrate the intramolecular hydrogen-bonding and chelation between a cadmium ion and the *ortho*-dihydroxy unit, and (b) synthesis and structure of COF-ETTA-2,3-Dha.

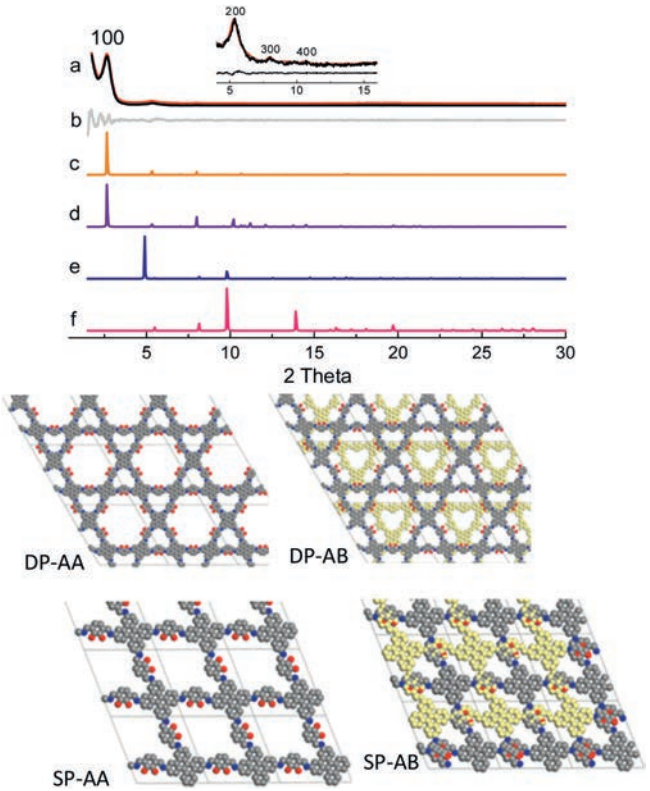

Fig. 1. Top: (a) experimental (black) and refined (red) PXRD patterns of COF-ETTA-2,3-Dha, (b) difference plot between the experimental and refined PXRD patterns, and simulated PXRD patterns for (c) DP-AA, (d) DP-AB, (e) SP-AA, and (f) SP-AB structures. Bottom: Illustrations of AA and AB stackings of dual-pore and single-pore COFs.

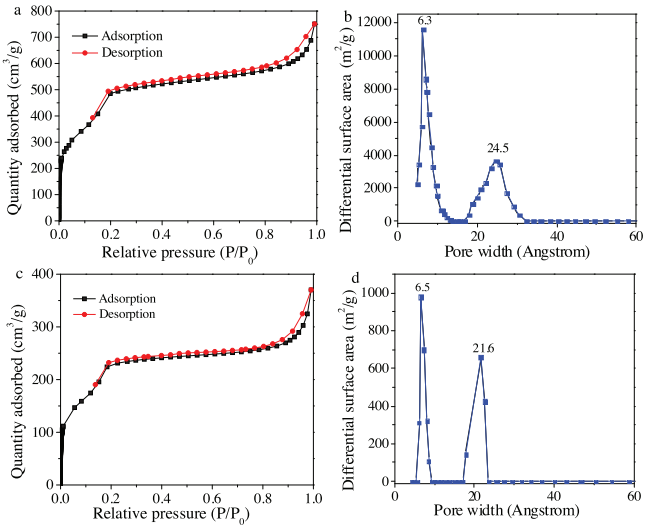

Fig. 2. (a) N_2 adsorption and desorption isotherm curve and (b) pore size distribution profile of the dual-pore COF-ETTA-2,3-Dha. (c) N_2 adsorption and desorption isotherm curve and (d) pore size distribution profile of COF-ETTA-2,3-Dha-Cd.

patterns were simulated (Figs. 1c–f and Table S2 in Supporting information). The comparison between the experimentally observed (Fig. 1a) and the simulated PXRD patterns clearly indicates that the as-prepared COF is the dual-pore one. As shown in Fig. 1a, a strong peak corresponding to the (100) diffraction is observed at 2 $\theta = 2.66°$. In addition, diffraction peaks at 5.32°, 8.01° and 10.65° are also observed, which are assignable to the diffractions of the (200), (300) and (400) facets, respectively. These peaks match the simulated PXRD pattern of the dual-pore COF quite well. Theoretical calculations suggest that the COF should adopt AA stacking, as the AB stacking has higher total energy than that of AA stacking (798.0 *vs.* 30.0 kcal/mol). Pawley refinement gives the unit-cell parameters of a = b = 38.30 Å, c = 5.26 Å, $\alpha = \beta = 90°$ and $\gamma = 120°$, with $R_{wp} = 3.71\%$ and $R_p = 2.72\%$. The difference plot reveals that the refined PXRD pattern nearly reproduces the experimental one (Fig. 1b), indicating the simulated model matches well with the experimental result.

Another key evidence to support the dual-pore COF structure is from the nitrogen adsorption-desorption experiment (Fig. 2a). The entire isotherm curve is quite similar to those previously observed for the dual-pore COFs with the same topological structure [19], indicating the presence of micropores and mesopores in the material. Its Brunauer–Emmett–Teller (BET) surface area was estimated from the isotherm data in the range of $P/P_0 = 0.05–0.3$, which afforded a value of 1476.5 m^2/g (Fig. S5 in Supporting information). The total pore volume of the COF was calculated at $P/P_0 = 0.99$ to be 0.91 cm^3/g. The pore size distribution (PSD) of COF-ETTA-2,3-Dha was estimated using nonlocal density functional theory (NLDFT), which revealed two main pore size distributions centered at 6.3 and 24.5 Å, respectively (Fig. 2b). These values are very close to the theoretical values derived from the simulated crystal structure, which are 5.9 and 26.3 Å for the triangular micropores and the hexagonal mesopores, respectively. On the basis of the PXRD data and the nitrogen sorption results, the dual-pore structure is corroborated for COF-ETTA-2,3-Dha.

The chemical stability of COF-ETTA-2,3-Dha in aqueous solutions under neutral, acidic, and basic conditions was evaluated by dispersing the COF samples in distilled water, aqueous HCl (3 mol/L) and NaOH (3 mol/L) solutions at 25 °C for 12 h, respectively. Prior to the PXRD analyses, the samples were separated by filtration, washed several times with distilled water, and then dried under vacuum at 120 °C for 3 h. Compared with that of the pristine COF, no obvious changes in the PXRD patterns are observed for the three samples (Fig. S6 in Supporting information), indicating that COF-ETTA-2,3-Dha has excellent resistance to water, acids, and bases. Its high stability against hydrolysis could be attributed to the intramolecular hydrogen-bonding interactions. As revealed by the previous work [17b,20], such interactions suppress the torsion of the edge unit and thus planarize the COF layers. As a result, the interlayer interactions are enhanced to stabilize the COF.

In view of the high surface area, periodically distributed nanosized channels, high chemical stability, and a large number of accessible ortho-dihydroxyl binding sites in COF-ETTA-2,3-Dha. Its capability as an adsorbent for adsorptive removal of Cd(II) from aqueous solutions was examined. The impact of contact time on Cd(II) adsorption was firstly studied at 298 K under a neutral condition. The successful adsorption of Cd(II) by COF-ETTA-2,3-Dha was revealed by energy-dispersive X-ray (EDX) analysis (Fig. S7 in Supporting information). Samples at different time intervals were collected and analyzed with inductively coupled plasma optical emission spectrometry (ICP-OES) to determine the adsorption amounts of Cd(II). As shown in Fig. 3a, the adsorption quantity increases rapidly during the early stage, with Cd uptakes of 39.6 mg/g at 1 min and 95.6 mg/g at 20 min, and then reaches a steady state after 60 min, at which point saturated adsorption of 116 mg/g is attained. To the best of our knowledge, it represents one of the highest values reported for the adsorption of Cd(II) so far (Table S1 in Supporting information). The excellent performance of COF-ETTA-2,3-Dha could be attributed to the abundant facilely accessible chelating sites of the catechol segment on the channel walls of the crystalline COF. The effect of solution pH on the

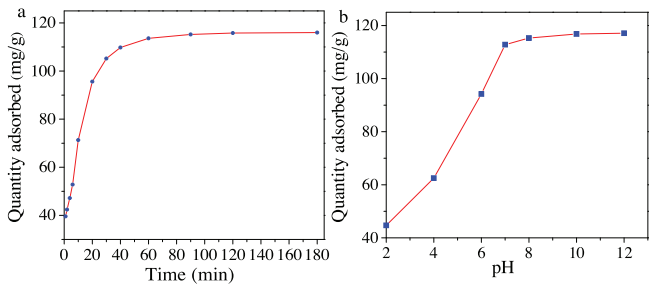

Fig. 3. (a) Time profile of Cd(II) adsorption with COF-ETTA-2,3-Dha under pH 7 and (b) impact of pH on the capture of Cd(II).

adsorption of Cd(II) was also investigated. As shown in Fig. 3b, the adsorption efficiency of the COF decreases upon decreasing the solution pH. By contrast, the neutral condition is favorable for Cd(II) adsorption and alkaline environments are even better. It is reasonable because the nitrogen atoms of imine bonds and hydroxyl groups might be partially protonated under acidic conditions and the extent of protonation increases with the decrease of pH. As a result, the chelating affinity of oxygen atoms to Cd(II) is weakened. Under neutral and basic conditions, such protonation is inhibited and thus pH does not exert significant influence on the adsorption capacity.

The Cd(II)-captured COF-ETTA-2,3-Dha (termed COF-ETTA-2,3-Dha-Cd) was characterized using FTIR spectroscopy and PXRD analysis (Figs. S8 and S9 in Supporting information). The bending vibration of O—H shifted from 1359.2 of the as-synthesized COF to 1358.0 cm^{-1} and the crystallinity just slightly attenuated after the Cd(II) adsorption. The N_2 adsorption and desorption isotherm curves of the COF before and after the adsorption of Cd(II) are almost the same in shape (Figs. 2a and c), suggesting retainment of the framework structure. However, the BET surface area of COF-ETTA-2,3-Dha-Cd is 783.6 m^2/g (Fig. S5b in Supporting information), just reaching half of that of the pristine COF. Moreover, it is also found that the total pore volume (at $P/P_0 = 0.99$) of the COF decreases to 0.40 cm^3/g after the adsorption of Cd(II). The PSD analysis of COF-ETTA-2,3-Dha-Cd reveals two main pore size distributions centered at 6.5 and 21.6 Å, respectively (Fig. 2d). Compared with the pristine COF, the pore size of the micropores is almost no change. By contrast, the pore diameter of the mesopores becomes smaller after the uptake of Cd(II), suggesting that Cd(II) ions might be mainly trapped in the mesoporous channels.

Recyclability of adsorbents is critical to their practical applications. The recyclability test of COF-ETTA-2,3-Dha reveals that it can be facilely regenerated from the Cd(II)-adsorbed COF by successively rinsing with an aqueous HCl solution (3 mol/L) and water, and the regenerated COF is then ready for the next round Cd(II) removal after drying. Notably, COF-ETTA-2,3-Dha retains 94% of the original cadmium capacity even after being used for five times (Fig. 4a). The maintenance of structural integrity after four

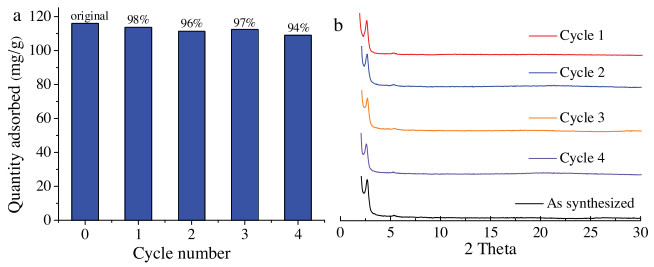

Fig. 4. (a) Cycle performance for Cd(II) removal by COF-ETTA-2,3-Dha in aqueous solution (pH 7) and (b) PXRD patterns of the COF after being used for different cycles.

adsorption/elution cycles is clearly evidenced by powder X-ray diffraction studies, which show almost no change in the PXRD pattern of each run (Fig. 4b), again indicating the extremely high chemical stability of the COF in aqueous solutions.

In summary, a novel heteropore COF has been developed as an adsorbent for adsorptive removal of cadmium from aqueous solutions. Thanks to the intramolecular hydrogen-bonding interactions introduced by catechol segment into the structural design, the COF exhibits extremely high chemical stability against water under various pH conditions. The design also endows the COF with many advantages including hierarchical porosity, high crystallinity, large specific surface area (1476.5 m^2/g), and abundant metal ions chelating sites which are facilely accessible. Benefiting from these advantages, a very rapid adsorption process (39.6 mg/g at 1 min and 95.6 mg/g in 20 min) and a remarkable cadmium absorption capacity of 116 mg/g are attained for the COF. Moreover, this material also displays good recyclability, which can be easily regenerated and used repeatedly with just a slight decrease in the uptake capacity. This work not only demonstrates the great potential of COFs for capturing water contaminants but also develops an instructive strategy for further design of high-performance adsorbents for adsorptive removal of heavy metal ions from wastewater.

Acknowledgments

We thank the National Natural Science Foundation of China (No. 21725404), Shanghai Scientific and Technological Innovation Project (No. 18JC1410600), and the Strategic Priority Research Program of the Chinese Academy of Sciences (No. XDB20000000) financial support.

Appendix A. Supplementary data

Supplementary material related to this article can be found, in the online version, at doi:https://doi.org/10.1016/j.cclet.2019.06.050.

References

[1] (a) R.P. Schwarzenbach, B.I. Escher, K. Fenner, et al., Science 313 (2006) 1072–1077;
(b) M.P. Waalkes, J. Inorg, Biochem. 79 (2000) 241–244;
(c) M. Hua, S. Zhang, B. Pan, et al., J. Hazard. Mater. 211–212 (2012) 317–331;
(d) P. Miretzky, A.F. Cirelli, J. Hazard. Mater. 167 (2009) 10–23;
(e) M.T. Hayat, M. Nauman, N. Nazir, S.Ali N. Bangash, Environmental hazards of cadmium: past, present, and future, in: M. Hasanuzzaman, M.N.V. Prasad, M. Fujita (Eds.), Cadmium Toxicity and Tolerance in Plants, Academic Press, New York, 2019, pp. 163–183;
(f) H. Liu, G. Liu, Z. Yuan, et al., Mar. Pollut. Bull. 140 (2019) 388–394;
(g) P.K. Samantaray, S. Baloda, G. Madras, S. Bose, J. Mater. Chem. A 6 (2018) 16664–16679.
[2] (a) H. Yamada, T. Miyahara, Y. Sasaki, Mutat. Res. Lett. 302 (1993) 137–145;
(b) I.A. Darwish, D.A. Blake, Anal. Chem. 73 (2001) 1889–1895;
(c) K. Nogawa, E. Kobayashi, Y. Okubo, Y. Suwazono, Biometals 17 (2004) 581–587;
(d) S. Khan, Q. Cao, Y.M. Zheng, Y.Z. Huang, Y.G. Zhu, Environ. Pollut. 152 (2008) 686–692;
(e) R. Zha, R. Nadimicherla, X. Guo, J. Mater. Chem A 2 (2014) 13932–13941.
[3] (a) S. Rodrigues, N. Munichandraiah, A.K. Shukla, J. Power Sources 87 (2000) 12–20;
(b) S. Ghatak, G. Chakraborty, M. Sinha, S.K. Pradhan, A.K. Meikap, Physica B 406 (2011) 3261–3266.
[4] (a) C. Zhu, Y. Guo, Y. Yang, et al., J. Environ. Eng. Technol. 8 (2018) 58–64;
(b) Y. Lan, R. Liang, X. Zhao, et al., Acta Sci. Circumstantiae 37 (2017) 3602–3612.
[5] (a) A. Özverdi, M. Erdem, J. Hazard. Mater. B 137 (2006) 626–632;
(b) J. Koelmel, M.N.V. Prasad, G. Velvizhi, S.K. Butti, S.V. Mohan, Metalliferous waste in India and knowledge explosion in metal recovery techniques and processes for the prevention of pollution, in: M.N.V. Prasad, K. Shih (Eds.), Environmental Materials and Waste, Academic Press, New York, 2016, pp. 339–390;
(c) D. Purkayastha, U. Mishra, S. Biswas, J. Water Process. Eng. 2 (2014) 105–128;
(d) F. Fu, Q. Wang, J. Environ. Manag. 92 (2011) 407–418.

[6] (a) J. Shao, J.D. Gu, L. Peng, et al., J. Hazard. Mater. 272 (2014) 83–88;
(b) M.Q. Jiang, X.Y. Jin, X.Q. Lu, Z.L. Chen, Desalination 252 (2010) 33–39;
(c) P. Pavasant, R. Apiratikul, V. Sungkhum, et al., Bioresour. Technol. 97 (2006) 2321–2329;
(d) Z. Feng, S. Zhu, D.R. Martins de Godoi, A.C.S. Samia, D. Scherson, Anal. Chem. 84 (2012) 3764–3770.
[7] (a) E. Samper, M. Rodríguez, M.A. De la Rubia, D. Prats, Sep. Purif. Technol. 65 (2009) 337–342;
(b) J.H. Huang, G.M. Zeng, C.F. Zhou, et al., J. Hazard. Mater. 183 (2010) 287–293;
(c) D.J. Ennigrou, L. Gzara, M.R. Ben Romdhane, M. Dhahbi, Desalination 246 (2009) 363–369.
[8] (a) L.E. Kanagy, B.M. Johnson, J.W. Castle, J.H. Rodgers Jr., Bioresour. Technol. 99 (2008) 1877–1885;
(b) H.A. Qdais, H. Moussa, Desalination 164 (2004) 105–110.
[9] (a) A. Üçer, A. Uyanik, Ş.F. Aygün, Sep. Purif. Technol. 47 (2006) 113–118;
(b) B.E. Reed, S. Arunachalam, B. Thomas, Environ. Prog. Sustain. 13 (1994) 60–64;
(c) B. Xiao, K.M. Thomas, Langmuir 21 (2005) 3892–3902.
[10] (a) J.L. Weidman, R.A. Mulvenna, B.W. Boudouris, W.A. Phillip, ACS Appl. Mater. Interfaces 9 (2017) 19152–19160;
(b) M.X. Tan, Y.N. Sum, J.Y. Ying, Y. Zhang, Energy Environ. Sci. 6 (2013) 3254–3259;
(c) H. Zhu, X. Tan, L. Tan, et al., ACS Sustain. Chem. Eng. 6 (2018) 5206–5213.
[11] (a) Y. Wang, G. Ye, H. Chen, et al., J. Mater. Chem. A 3 (2015) 15292–15298;
(b) J. Zhang, Z. Xiong, C. Li, C. Wu, J. Mol. Liq. 221 (2016) 43–50;
(c) C. Liu, P. Wang, X. Liu, et al., Chem. -Asian J. 14 (2019) 261–268;
(d) J. Li, X. Wang, G. Zhao, et al., Chem. Soc. Rev. 47 (2018) 2322–2356.
[12] (a) A.P. Côté, A.I. Benin, N.W. Ockwig, M. O'Keeffe, A.J. Matzger, O.M. Yaghi, Science 310 (2005) 1166–1170;
(b) S.Y. Ding, W. Wang, Chem. Soc. Rev. 42 (2013) 548–568;
(c) P.J. Waller, F. Gándara, O.M. Yaghi, Acc. Chem. Res. 48 (2015) 3053–3063;
(d) S. Kandambeth, K. Dey, R. Banerjee, J. Am. Chem. Soc. 141 (2019) 1807–1822.
[13] (a) M.S. Lohse, T. Bein, Adv. Funct. Mater. 28 (2018) 1705553;
(b) Y. Song, Q. Sun, B. Aguila, S. Ma, Adv. Sci. 6 (2019) 1801410;
(c) N. Huang, P. Wang, D. Jiang, Nat. Rev. Mater. 1 (2016) 16068;
(d) M.X. Wu, Y.W. Yang, Chin. Chem. Lett. 28 (2017) 1135–1143.
[14] (a) S.Y. Ding, M. Dong, Y.W. Wang, et al., J. Am. Chem. Soc. 138 (2016) 3031–3037;
(b) N. Huang, L. Zhai, H. Xu, D. Jiang, J. Am. Chem. Soc. 139 (2017) 2428–2434;
(c) Q. Sun, B. Aguila, J. Perman, et al., J. Am. Chem. Soc. 139 (2017) 2786–2793;
(d) K. Leus, K. Folens, N.R. Nicomel, et al., J. Hazard. Mater. 353 (2018) 312–319;
(e) Q. Lu, Y. Ma, H. Li, et al., Angew. Chem. Int. Ed. 57 (2018) 6042–6048;
(f) Z.A. Ghazi, A.M. Khattak, R. Iqbal, et al., New J. Chem. 42 (2018) 10234–10242;
(g) F.Z. Cui, R.R. Liang, Q.Y. Qi, G.F. Jiang, X. Zhao, Adv. Sustain. Syst. (2019) 1800150.
[15] (a) X.Y. Yang, L.H. Chen, Y. Li, et al., Chem. Soc. Rev. 46 (2017) 481–558;
(b) S. Lopez-Orozco, A. Inayat, A. Schwab, T. Selvam, W. Schwieger, Adv. Mater. 23 (2011) 2602–2615;
(c) Y. Li, Z.Y. Fu, B.L. Su, Adv. Funct. Mater. 22 (2012) 4634–4667.
[16] R.R. Liang, X. Zhao, Org. Chem. Front. 5 (2018) 3341–3356.
[17] (a) D.B. Shinde, S. Kandambeth, P. Pachfule, R.R. Kumar, R. Banerjee, Chem. Commun. 51 (2015) 310–313;
(b) A. Halder, S. Kandambeth, B.P. Biswal, et al., Angew. Chem. Int. Ed. 55 (2016) 7806–7810.
[18] Dassault Systèmes BIOVIA, Materials Studio 8.0, Dassault Systèmes San Diego, (2014) .
[19] (a) T.Y. Zhou, S.Q. Xu, Q. Wen, Z.F. Pang, X. Zhao, J. Am. Chem. Soc. 136 (2014) 15885–15888;
(b) Z.F. Pang, T.Y. Zhou, R.R. Liang, Q.Y. Qi, X. Zhao, Chem. Sci. 8 (2017) 3866–3870.
[20] X. Chen, M. Addicoat, E. Jin, et al., J. Am. Chem. Soc. 137 (2015) 3241–3247.